REGULAR PAPER

Optimal Design of Gerotor Profile with Lemniscate Lobe Shape for Noise Reduction

Changhyun Lee[1] · Hyoseong Jang[1] · Hyoseo Kwak[2] · Gunyoung Park[1] · Chul Kim[1,2]

Abstract

Since gerotor oil pump has a simple structure and has a higher discharge per cycle than other types of pumps with the same size, it has advantage for miniaturization, so it is widely used as the source of lubricant for engine lubrication of automobiles or as the hydraulic source of automatic transmissions. In order to improve the fuel efficiency and reduce the noise of gerotor oil pumps, optimization of the tooth profile is required. Thus, in this study, 2-Ex_Lemniscates; 2-expanded lemniscates curve, was developed as a new lobe shape, and theoretical equations for generating a rotor profile used as the tooth profile of the outer rotor were derived. In addition, new algorithm has removed 'cusp' generated in outer rotor and made uniform clearance between outer and inner rotors by applying translational movement of the x and y axes along with the expansion and rotation, and using automatic design program, optimal profile was proposed based on the analysis of performance parameters for about 2.6 million tooth profiles. The experimental results showed that the developed 2-Ex_Lemniscates oil pump showed that the flow rate at 2500 rpm was increased by about 2.9%, and average SPL (2000–3000 rpm) and pressure irregularity were decreased by 3.3% and 16.9%, respectively.

List of Symbols

α	Phase angle of outer pitch circle to find contact points
α'	Phase angle of inner pitch circle to find contact points
η	Rotation angle of the expanded lemniscate curve
θ	Parameter angle of lemniscate curve
θ'	Parameter angle of point on 2-Ex_lemniscate curve that satisfies orthogonal condition
ρ	Distance from center of outer rotor to contact point
ρ_{fluid}	Fluid density at 20 °C (845 kg/m^3)
b	Axial thickness of rotor
d	Distance of parallel translation considering pitch diameter
e	Amount of eccentricity between inner rotor and outer rotor
h	Distance of horizontal translation for symmetry transformation
k_1	Scale factor of the lobe shape about the x-axis
k_2	Scale factor of the lobe shape about the y-axis
O_e	Center of inner rotor
O_i	Center of inner rotor
O_o	Center of outer rotor
r_1	Radius of inner rotor
r_2	Radius of outer rotor
ss_1	Value of specific slipping of inner rotor
ss_2	Value of specific slipping of outer rotor
$\vec{v_1}$	Direction vector from a point on the lobe (x_n, y_n) to the pitch point (P_a)
$\vec{v_2}$	Tangent vector at a point (x_n, y_n) on the 2-Ex_Lemniscate curve
x_{move}	Distance of parallel translation for rotation transformation
$x_{move,2}$	Distance of parallel translation for independence of design parameter 'd'
z_1	The number of teeth of inner rotor
z_2	The number of teeth of outer rotor

✉ Chul Kim
chulki@pusan.ac.kr

1 School of Mechanical Engineering, Pusan National University, Busan, South Korea

2 School of Mechanical and Automotive Engineering, Youngsan University, 288, Junam-ro, Yangsan-si, Republic of Korea

1 Introduction

Gerotor oil pump has advantages for miniaturization since it has a higher discharge per cycle in comparison with vane pumps or gear pumps with the same size. Inner and outer rotors are easy to process because they are sintered products with a simple structure, and gerotor pump shows little change in efficiency even when used for a long time because of a small relative motion between the teeth. In addition, the gerotor oil pump produces low noise and has good suction performance. Thus, it is widely used in hydraulic systems, such as the supply system of lubricants in automotive engines and the hydraulic source for automatic transmissions. In order to improve fuel efficiency and noise, which are major issues in the automotive industry, the design of a new tooth profile for the gerotor oil pump with high performance and low noise characteristics is required [1–9].

Previous studies on gerotor profile design have mostly focused on ellipse or trochoid curves (cycloid, epitrochoid and hypotrochoid) [1–5, 9]. Hsieh compared three different design curves: an epitrochoid curve, a hypotrochoidal curve, and a curve made by continuously connecting the epicycloid and hypocycloid. The area efficiencies of three profiles were theoretically compared in a non-undercutting situation, and the distance of inward offset about inner rotor that can cause cusp and can affect area efficiency was considered [1]. Ravari proposed the optimization method of an epitrochoidal gerotor considering volumetric, dynamic and geometric properties for the reduction of flow irregularity and wear flow. The optimization results of commercial pumps were based on theoretical analysis, and it was concluded that using the greater number of outer rotor teeth improved wear of teeth and that irregularity was improved when number of outer rotor teeth was odd value, not even value [2]. Bonandrini et al. [3] also parameterized an epitrochoidal profile for internal rotary pumps to have superior flow-rate performance, and a tooth contact analysis was performed to consider possible transmission errors. Xiaohu et al. [4] tried to eliminate engaging limiting point for elliptical rotor profiles optimization. Gamez-Montero [5] designed trochoidal teeth considering maximum contact stress and volumetric characteristics. About the maximum contact stress, the significant parameters are the number of teeth and the minimum radius of curvature of the internal gear. Increase of the number of teeth makes teeth more sharp, producing high contact forces. Tessari et al. [9] aimed to design trochoidal profile with maximized volumetric and mechanical efficiency, considering leakage flow rate based on 72 CFD results. Rituraj and Vacca [6] proposed tooth tip leakage model by implementing CFD simulations and experiments in order to predict the leakage flow and to improve the volumetric efficiency. Cao et al. [7] designed a gerotor pump

with pulsation buffer and remarkably reduced pressure pulsation. Lee suggested 2-expanded cardioids gerotor, which had better performances in noise reduction and irregularity than 2-Ellipses previously developed, but the previous algorithm with expansion and rotation used in 2-expanded cardioids gerotor has generated 'cusp' in the outer rotor as shown in Figs. 1 and 2, so that it influenced in noise, irregularity and flowrate due to non-uniform clearance between outer rotor and inner rotor [8].

As shown in Fig. 2, 'cusp' always occurred by only rotation movement in previous study was removed due to the application of the new algorithm (rotation, translation movement), and the removal of 'cusp' from all the teeth of inner/outer rotor lets existing irregular clearance uniformed as shown in Fig. 2b, which is effective in mechanical noise reduction.

As shown in Fig. 3a, 2-Ex_Cardioid is excellent in terms of noise, compared to Ell1-Inv-Ell2, 2-Ellipses and cardioid_EX, because of the outer rotor gradually thickened according to the basic lobe shape and the tooth of the inner rotor thinned as shown in Fig. 3b. Based on the above result, the shape of lemniscate, a new curve that allows the tooth shape of the outer rotor to be designed more outward (outer rotor: thick, inner rotor: thin), compared to the previous lobe shapes (Epitrochoid, Cardioid, and Ellipse) as shown in Fig. 3b, was selected in the study to reduce noise.

Constitutive equations of the tooth profile were derived base on the designed outer lobe, and then inner and outer rotors with the new lobe shape (2-Ex_Lemniscates; 2-expanded lemniscates) were generated. An automatic program for generation of inner and outer rotors and a multi calculation program for calculating the performance parameters (flow rate, irregularity, contact stress, specific slipping and pressure angle) were developed using Matlab. The performance parameters to be influenced in noise have been established by experiments and studies carried out in our laboratory for a long time and the results are as follows; (irregularity > contact stress > specific slipping > pressure angle) Based on the above result, this study focuses on comparing the effect of noise by changing the flow characteristic caused by the inner lobe shape automatically generated according to the outer lobe shape using lemniscate curve and tries to find out the best lobe shape to reduce noise. Using the automatic programs, an optimal profile with 2-Ex_Lemniscates lobe shape was proposed, and its theoretical performances were compared with those of 2-Ex_Cardioids, which showed the best performance in previous study. In addition, oil pump prototype for the proposed 2-Ex_Lemniscates profile was manufactured with four profiles developed in previous studies (Existing Standard Profile, 2-Ellipses, 2-Ex_Cardioids, 2-Ex_Epitrochoids), and a performance test was conducted. As a result, compared to the previous optimal oil pump with 2-Ex_Cardioids, the new oil pump
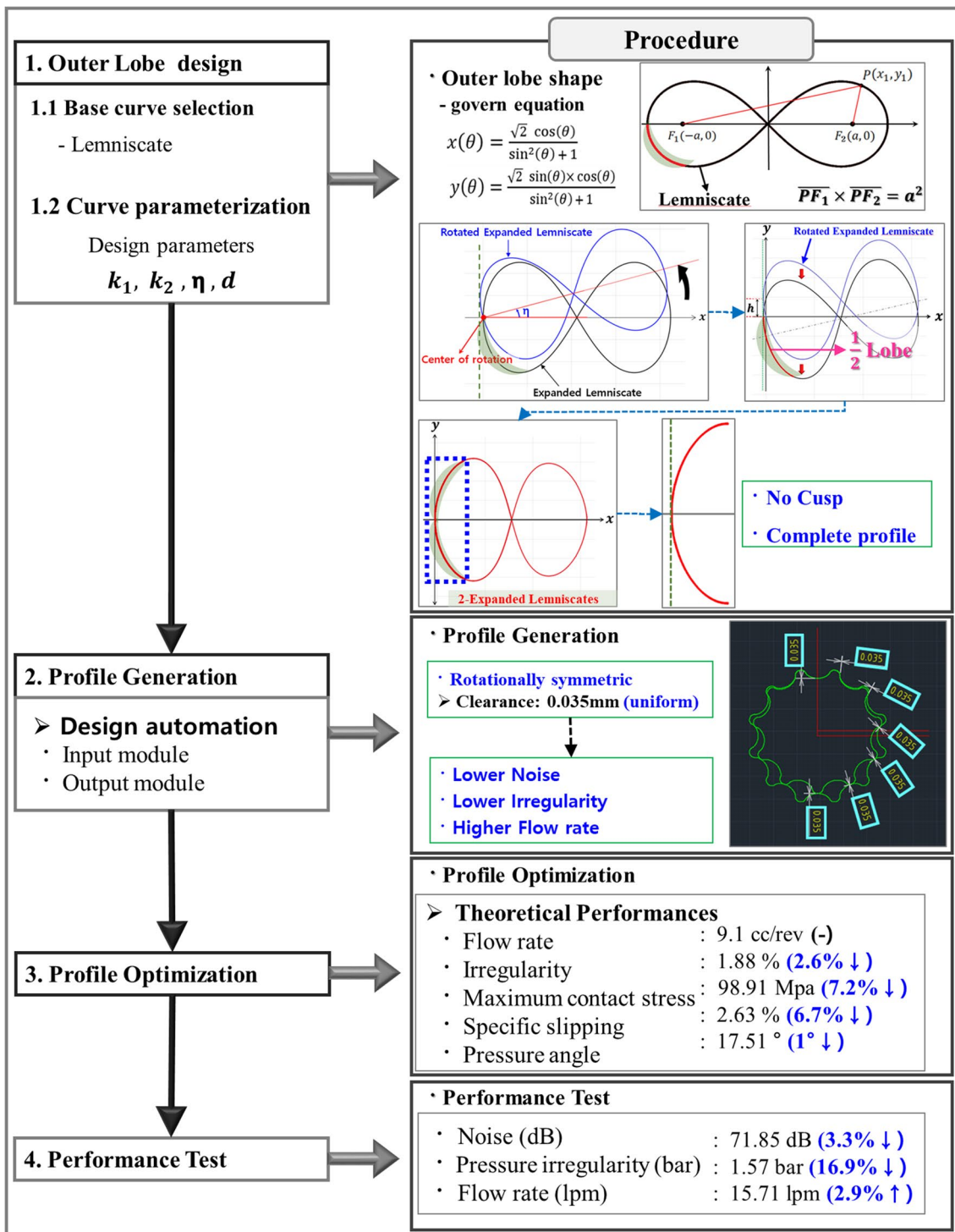
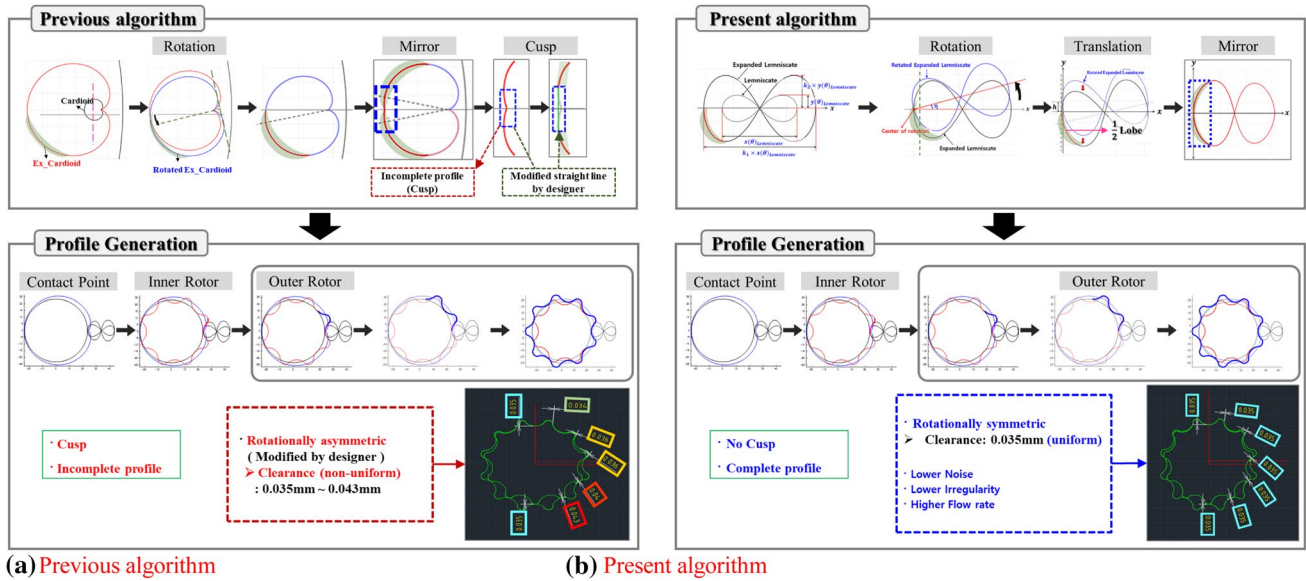**Fig. 1** Configuration of this study using technology tree
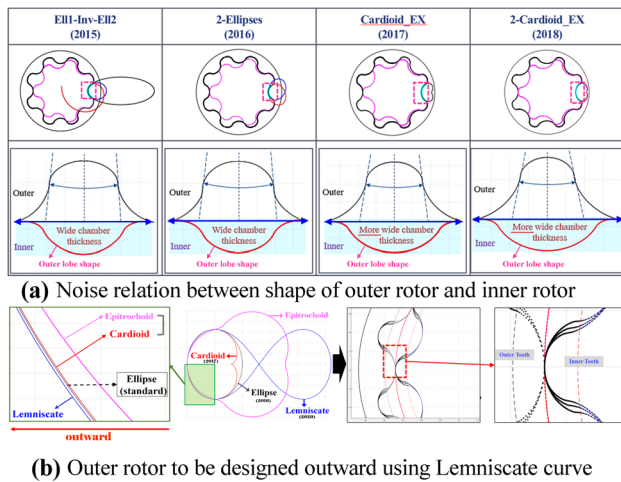
Fig. 2 Modified lobe generation algorithm

(a) Noise relation between shape of outer rotor and inner rotor

(b) Outer rotor to be designed outward using Lemniscate curve

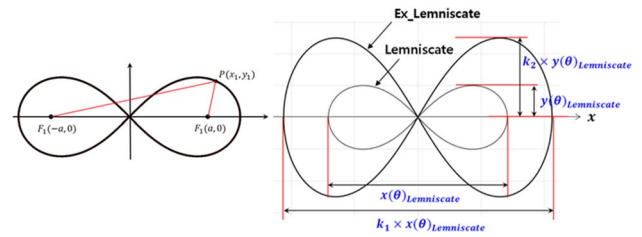**Fig. 3** Characteristic of lobe shape with lemniscate curve

Fig. 4 Lemniscate and Ex_Lemniscate curves

each point P on the curve. The shape of the curve is similar to the number 8 or symbol ∞, and its name is derived from Latin, meaning pendant ribbon.

In previous studies on the optimal design of the gerotor tooth profile, two curves-combined lobe shapes (2-Ellipses) tended to show better performance compared to a single lobe shape (Circle, Ellipse and Expanded Cardioid) or three or more curves-combined lobe shapes (EIE, 3-Ellipse). In particular, the tooth profile with a 2-Expanded Cardioids lobe shape showed better performance than the tooth profile with a 2-Ellipses lobe shape in terms of noise reduction.

A constitutive equation was generated using the lemniscate of Bernoulli as shown in Eq. (1), and the expanded lemniscate curve (Ex_Lemniscate) was generated by multiplying the x-coordinate and y-coordinate by 'k$_1$' and 'k$_2$', respectively, as shown in Eq. (2) and Fig. 4.

$$\left(x^2 + y^2\right)^2 = 2a^2\left(x^2 - y^2\right) \tag{1}$$

showed that the flow rate at 2500 rpm was increased by about 2.9%, and average SPL (2000–3000 rpm) and pressure irregularity were decreased by 3.3% and 16.9%, respectively.

2 Design of Lobe Shape with a 2-Ex_Lemniscates Curve

2.1 Design of Outer Lobe Shape

The lemniscate curve was first designed in 1694 by Jacob Bernoulli. Geven two focal points **F**1 and **F**2 with a distance of 2**a**, it is a curve on a plane satisfying $\boldsymbol{PF}_1 \cdot \boldsymbol{PF}_2 = \boldsymbol{a}^2$ for

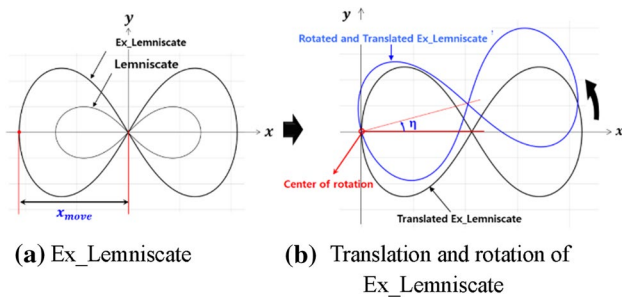**(a)** Ex_Lemniscate **(b)** Translation and rotation of Ex_Lemniscate

Fig. 5 Translation and rotation transformations of Ex_Lemniscate curve

$$x_1(\theta) = \frac{\sqrt{2}\cos(\theta)}{\sin^2(\theta)+1}, \quad y_1(\theta) = \frac{\sqrt{2}\sin(\theta)\times\cos(\theta)}{\sin^2(\theta)+1} \quad (2)$$

$$x_2(\theta) = k_1 \times x_1, \quad y_2(\theta) = k_2 \times y_1$$

2-Ex_Lemniscates curve was newly devised by the combination method using translation, rotation and symmetry algorithms. To use the left end point on the x-axis as the center of rotation shown in Fig. 5a, Ex_Lemniscate curve was translated to the origin point by 'x_{move}' and rotated by 'η' about the origin, as shown in Fig. 5b. The translation and rotation transformations are expressed as Eq. (3).

$$x3, rotated(\theta) = (x2 + xmove) \times cos(\eta) - y2 \times sin(\eta)$$
$$y3, rotated(\theta) = (x2 + xmove) \times sin(\eta) + y2 \times cos(\eta) \quad (3)$$

Figure 6a shows the Ex_Lemniscate lobe shape designed by the expansion, and Fig. 6b shows the lobe shape newly designed by rotation transformation. Since Fig. 6b shows a 1/2 model of the tooth profile of the outer rotor, it is required to rotate the Ex-Lemniscate by '-η', which is the rotation angle in the opposite direction to create full model, and it was subsequently designed using the symmetry algorithm.

In order to generate a full model of tooth profile using the 1/2 lobe shape in Fig. 6, the curve was translated parallel to the y-axis by 'h' so that the point with a slope of '∞'

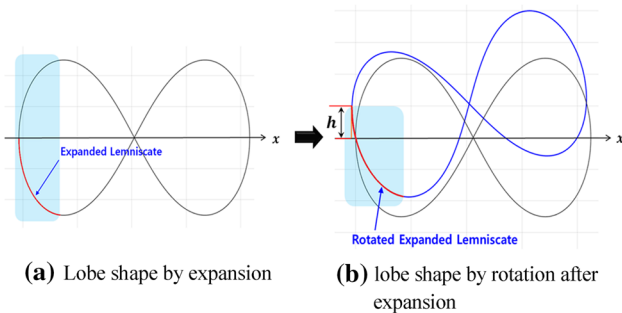**(a)** Lobe shape by expansion **(b)** lobe shape by rotation after expansion

Fig. 6 Lobe shapes by expansion and rotation after expansion

(a) Rotated Ex_Lemniscate **(b)** Translation parallel to y-axis

(c) Translation parallel to x-axis **(d)** Symmetry to x-axis

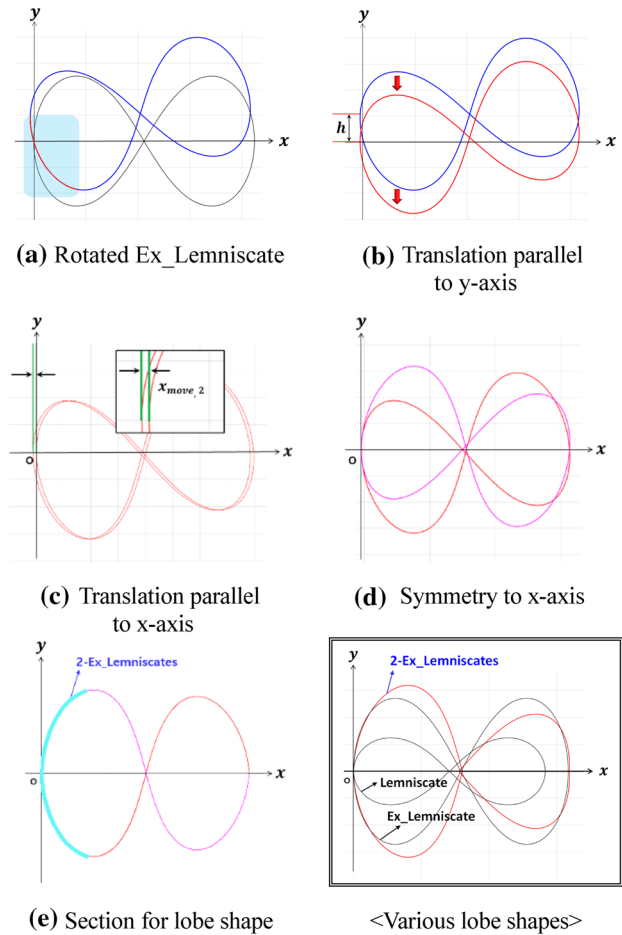**(e)** Section for lobe shape <Various lobe shapes>

**Fig. 7** Design process for 2-Ex_Lemniscates lobe shape

after rotation with respect to the x-axis in Fig. 7a would be on the x-axis as shown in Fig. 7b, and the curve generated is represented by Eq. (4). At this time, the left end point of the generated curve on the x-axis is moved farther away from the y-axis as shown in Fig. 7c, so the point on the x-axis is moved by '$x_{move,2}$' toward the origin, and the curve generated is expressed by Eq. (5), and the value of '$x_{move,2}$' changes according to the rotation angle 'η'. The other half of the lobe shape is obtained by moving it to be symmetry with respect to the x-axis as shown in Fig. 7d, e, and the equation is expressed as Eq. (6).
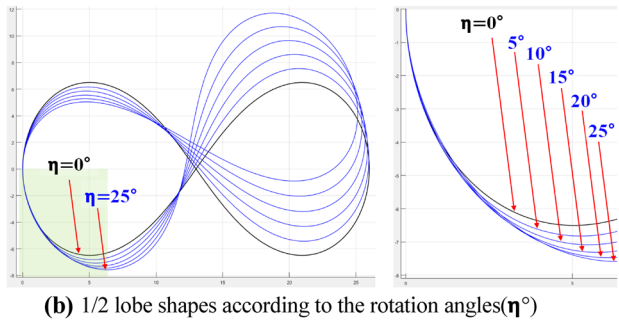
$$x_4(\theta) = x_{3,rotated}(\theta)$$
$$y_{4,Y-translation}(\theta) = y_{3,rotated}(\theta) - h \quad (4)$$

$$x_{5,X-translation}(\theta) = x_{4,translation} + x_{move,2}$$
$$y_{5,X-translation}(\theta) = y_{4,translation} \quad (5)$$
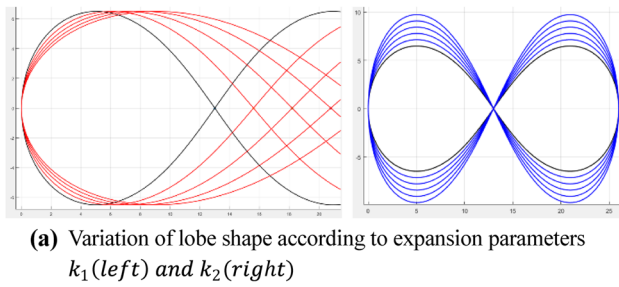
(a) Variation of lobe shape according to expansion parameters $k_1(left)$ and $k_2(right)$

(b) 1/2 lobe shapes according to the rotation angles($\eta°$)
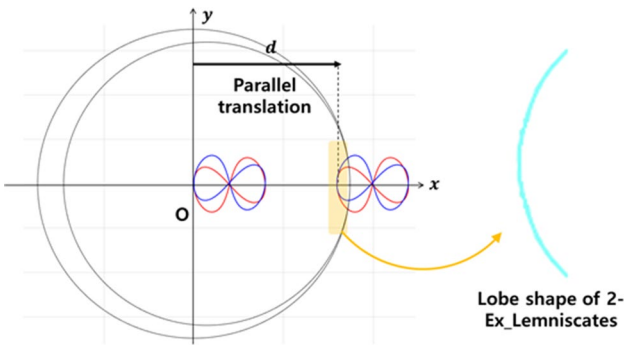
Fig. 8 Lobe shape variation according to k_1, k_2, $\eta°$

Fig. 9 Parallel translation of 2-Ex_Lemniscates

$$x_6(\theta) = x_{5,X-translation}$$
$$y_{6,symmetry}(\theta) = -y_{5,X-translation} \tag{6}$$

The 2-Ex_Lemniscates lobe generated as shown in Fig. 7e is obtained by expanding Lemniscate on the x and y axes according to the values of design parameters 'k_1' and 'k_2' and by rotating. In previous studies, as one type of curve (Ellipse, Cardioid, Epitrochoid, or Lemniscate) was selected, the lobe shape was limited to the initial curvature of the curve, but in this study, various lobe shape can be obtained from lemniscate curve since an independent curve can be designed for each angle of rotation. Additionally, Ex_Lemniscate curve corresponds to a 2-Ex_Lemniscates curve generated when 'η' = 0°. Figure 8 shows variation of lobe shape according to the design parameters: k_1, k_2 and $\eta°$.
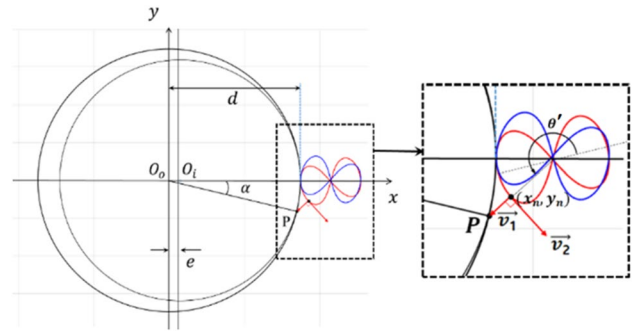

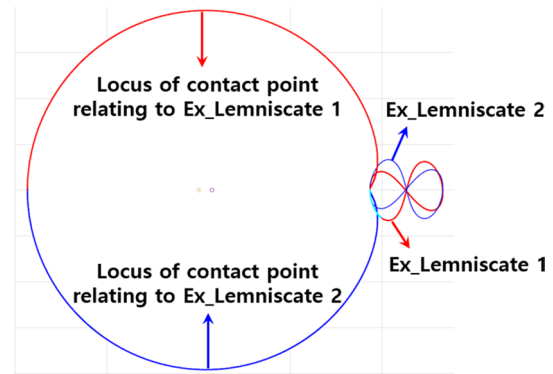**Fig. 10** Orthogonal condition to find contact point

Fig. 11 Locus of contact points of 2-Ex_Lemniscates

The 2-Ex_Lemniscates curve generated finally in Fig. 7e was translated by 'd' in the direction of the x-axis to generate the outer lobe shape with respect to the pitch circle of the outer rotor, as shown in Fig. 9, and this curve is expressed by Eq. (7). In Fig. 9, the origin 'O' is the center of the outer rotor, and 'd' is the distance of parallel translation of the outer lobe from 'O'.

$$x_{7-1,X-translation}(\theta) = x_{5,translation} + d$$
$$y_{7-1}(\theta) = y_{5,X-translation}(\theta) \tag{7}$$

$$x_{7-2,X-translation}(\theta) = x_{7-1}(\theta)$$
$$y_{7-2}(\theta) = -y_{7-1}(\theta)$$

2.2 Locus of Contact Points

The theory of Camus states that a common tangent line built at the tooth profile passes the pitch point in a contact point in order that a pair of gears to maintain a constant ratio of the angular velocity, the common normal must pass through the pitch point on the gear centerline at the contact point of two engaging teeth. According to the theory of Camus, the

common normal at the contact point must pass through the point '$P_{\alpha, 0 \leq \alpha \leq 360}$' on the pitch circle of the outer rotor, as shown in Fig. 10.

The angle (θ') makes the direction vector ($\vec{v_1}$) from a point on the lobe (x_n, y_n) to the pitch point (P_α) and the tangent vector ($\vec{v_2}$) to be perpendicular to each other, and it is found by the Newton-Rhapson method to satisfy the error range of 10^{-7}. The contact point (C) is determined by Eqs. (8)–(11), and the locus of the contact points is shown in Fig. 11. 'O_o' and 'O_i' are the centers of the outer and inner rotors, respectively, and 'e' represents eccentricity.

$$P(P_x, P_y) = (r_2 \cos \alpha, r_2 \sin \alpha)$$

$$\overrightarrow{v_{n,1}} = (P_x - x_n, P_y - y_n), \overrightarrow{v_{n,2}} = (dx_n, dy_n)$$

$$ff = \overrightarrow{v_{n,1}} \cdot \overrightarrow{v_{n,2}} = 0, \quad \theta' = \theta - \frac{ff}{dff}$$

$$C = \begin{pmatrix} x_c \\ y_c \end{pmatrix} = \begin{pmatrix} x_7(\theta') \times \cos(\alpha) - y_7(\theta') \times \sin(\alpha) \\ x_7(\theta') \times \sin(\alpha) + y_7(\theta') \times \cos(\alpha) \end{pmatrix} \tag{11}$$

2.3 Design of Inner and Outer Rotor Shape

Tooth profiles of inner and outer rotors are generated by Eqs. (12)–(14) as shown in Fig. 12. The contact points of the outer rotor are rotated clockwise by α' about the center (O_i) of the inner rotor to generate the inner rotor (x_{in}, y_{in}), and the contact points are rotated clockwise by α about the center (O_o) of the outer rotor to generate the outer rotor (x_{out}, y_{out}) as shown in Fig. 10. 'r_1' and 'r_2' represent radius of the pitch circles of the inner and outer rotors, respectively.
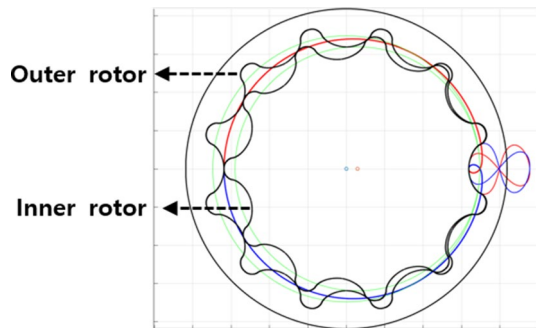
$$\alpha' = \frac{r_2}{r_1}\alpha, \quad (r_1 = z_1 \times e, \ r_2 = z_2 \times e) \tag{12}$$

$$\begin{pmatrix} x_{inner} \\ y_{inner} \end{pmatrix} = \begin{pmatrix} \cos \alpha' & -\sin \alpha' \\ \sin \alpha' & \cos \alpha' \end{pmatrix} \begin{pmatrix} x_c - e \\ y_c \end{pmatrix} + \begin{pmatrix} e \\ 0 \end{pmatrix} \tag{13}$$

$$\begin{pmatrix} x_{outer} \\ y_{outer} \end{pmatrix} = \begin{pmatrix} \cos \alpha & -\sin \alpha \\ \sin \alpha & \cos \alpha \end{pmatrix} \begin{pmatrix} x_c \\ y_c \end{pmatrix} \tag{14}$$

2.4 Performances of Gerotor

Flow rate (Q), which is the amount of the working fluid in the chamber, is calculated by Eq. (15), where A_{max} and A_{min} are maximum and minimum areas of the chamber, respectively, and 'b', 'ρ_{fluid}' and 'ω_1' are the thickness of the gerotor, density of the working fluid, and rotational speed of the inner rotor, respectively [8]. Flow rate irregularity (i) is proportional to the difference between the maximum area (q_{max}) and minimum area (q_{min}) of the chamber, as shown in Eq. (16).

$$Q = Z_1 (A_{max} - A_{min}) \rho_{fluid} \, bw_1 \tag{15}$$

$$i = \frac{q_{max} - q_{min}}{q_{average}} \tag{16}$$

Specific sliding is the ratio of sliding velocities on the plane passing through the contact point between two engaging gears. This is the difference between the tangential rolling velocity on the tooth profile and the velocity perpendicular to the line of action. Equation (17) shows the equations to calculate the values of specific slipping (ss$_1$ and ss$_2$) of inner and outer rotors, where 'v_1' and 'v_2' are the sliding velocities of inner and outer rotors, respectively

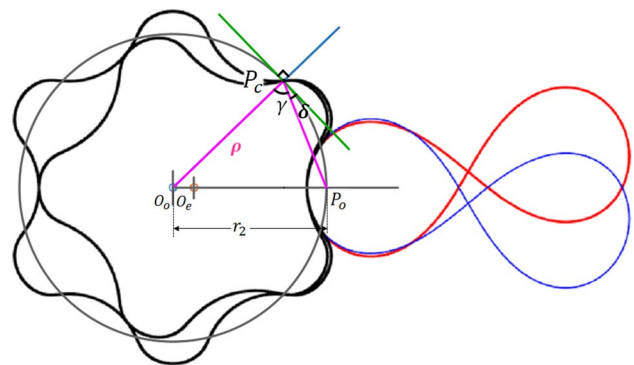**Fig. 12** Inner and outer rotors with 2-Ex_Lemniscates lobe shape

Fig. 13 Schematic model of pressure angle

$$ss_1 = \frac{|v_1 - v_2|}{v_1}, \quad ss_2 = \frac{|v_2 - v_1|}{v_2} \tag{17}$$

The pressure angle (δ) is the angle between the common tangent of engaging gears on the pitch circle and the common normal of the teeth in contact with each other, as shown in Fig. 13 and it is calculated by Eqs. (18)–(19).

$$\gamma = \cos^{-1}\left(\frac{\rho^2 + \overline{P_c P_o}^2 - r_2^2}{2 \, \overline{P_c P_o} \, \rho} \right) \tag{18}$$

$$\delta = 90° - \gamma \tag{19}$$

The contact stress (P_H) of two objects in relative motion is generally calculated by the equation for the Hertzian contact stress represented by Eq. (20). When the inner rotor comes into contact with the outer rotor, contact force is generated in opposite directions, causing contact stress. 'F' is the contact force applied to the inner rotor at the contact point, 'E' is the modulus of elasticity of the gerotor, 'b' is the tooth width, 'R' is the equivalent radius of curvature, and 'ρ_i' and 'ρ_o' are the radius of curvature of the inner and outer rotors, respectively.

$$P_H = \sqrt{\frac{FE}{2\pi bR}}, \quad R = \left(\frac{1}{\rho_i} + \frac{1}{\rho_o} \right)^{-1} \tag{20}$$

3 Optimal Design of 2-Ex_Lemniscates curve Lobe Shape

3.1 Development of Automatic Program

In order to find an optimal tooth profile, an automatic program, which shows shape of tooth profile according to the input design parameters and calculates performance parameters, was developed using the commercial numerical analysis software, MATLAB (R2017b, The MathWorks, Inc. Natick, Massachusetts, USA). Figure 14 shows GUI, which visually shows shape of tooth profile and the calculation results of performance parameters when the design parameters of the 2-Ex_Lemniscates lobe shape are entered. GUI consists of an input module (selection of lobe shape and input value of design parameter) and an output module (gerotor profile and performance parameters). In the input module, type of lobe shape is selected, and then the fixed design parameters (the number of teeth of the outer rotor, eccentricity, outer diameter of the outer rotor, and tooth width) and the variable design parameters ('d', 'k_1', 'k_2' and 'η') are entered. The tooth profiles of inner and outer rotors are generated in the

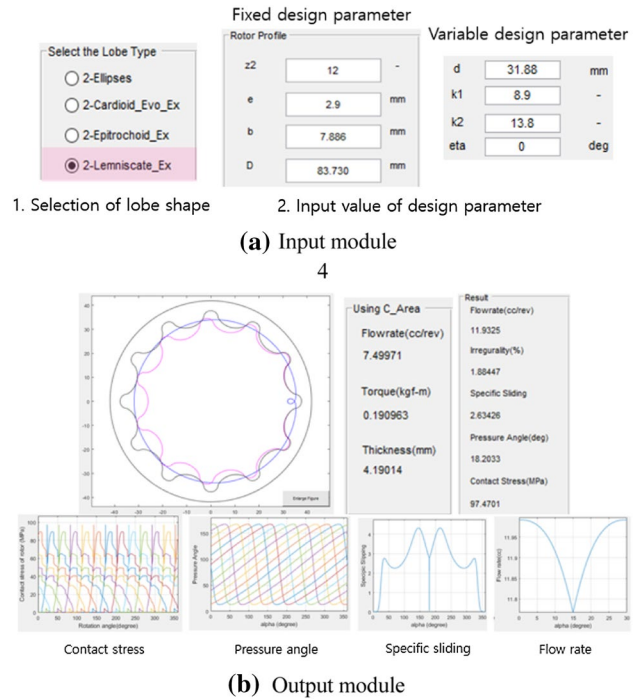
(a) Input module

(b) Output module

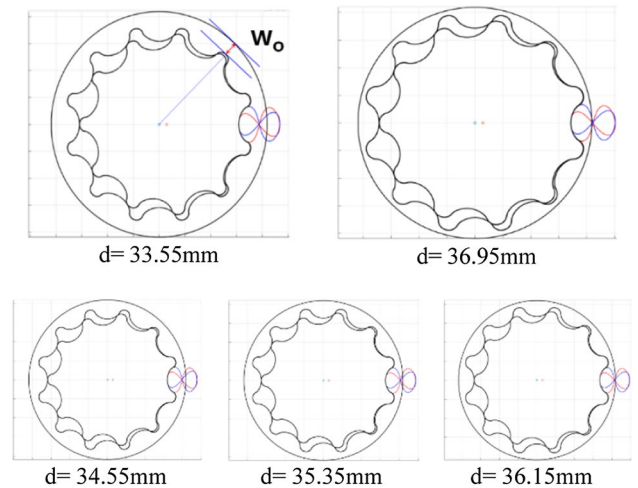**Fig. 14** GUI of automatic program for design of gerotor

Fig. 15 Gerotor profile by varying 'd' ($k_1 = 5.6$, $k_2 = 10.85$, $\eta = 13°$)

output module, and the performance parameters (flow rate, flow rate irregularity, contact stress, specific slipping and pressure angle) are automatically displayed on the screen.

The tooth profiles by varying the value of each variable design parameter ('d', 'k_1', 'k_2' and 'η') are shown in Figs. 14, 15, 16 and 17. As the value of 'd' increases, the outer lobe is generated in a more distant position in the radial direction, so the tooth thickness of the inner rotor generated is increased and radial thickness of the outer rotor (W_o) is decreased as shown in Fig. 15. The range (34.4–34.75 mm)
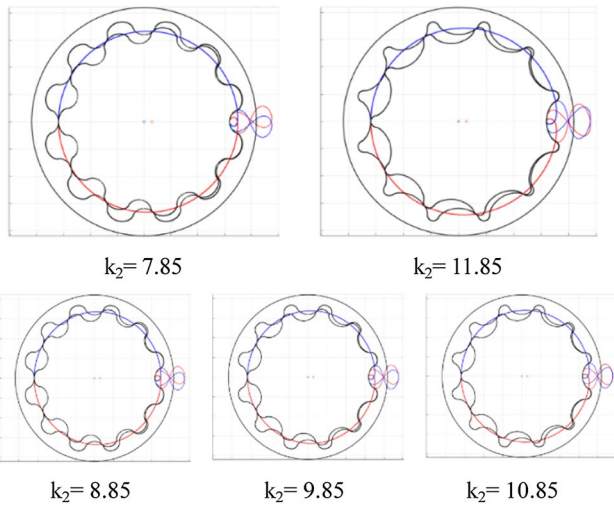
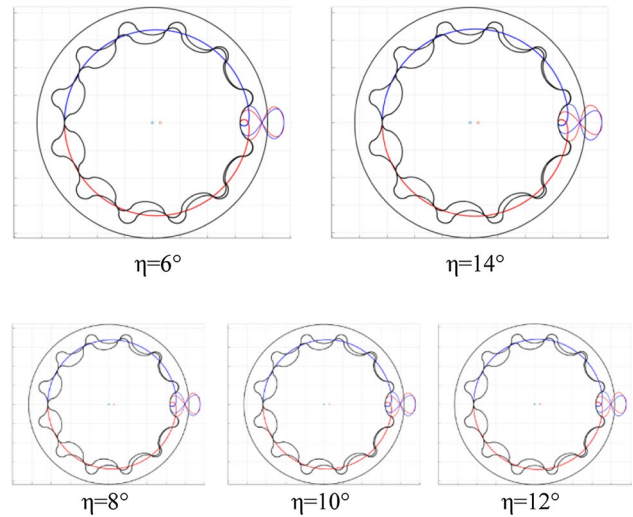Fig. 16 Gerotor profile by varying 'k_1'($d = 34.55$, $k_2 = 10.85$, $\eta = 13°$)

Fig. 18 Gerotor profile by varying 'η' ($d = 34.55$, $k_1 = 5.6$, $k_2 = 10.85$)
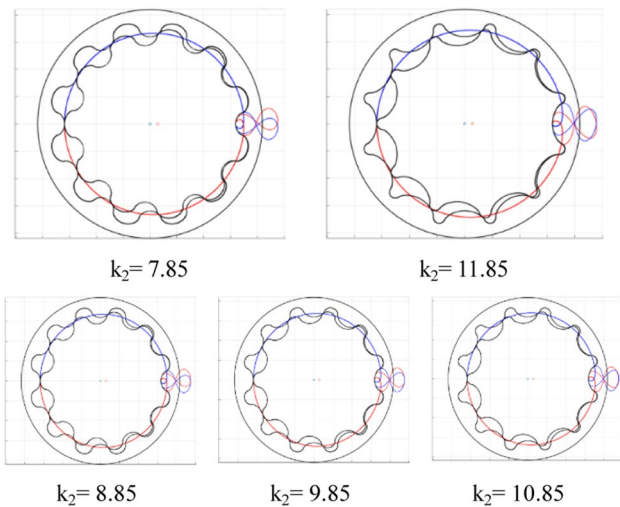
Fig. 17 Gerotor profile by varying 'k_2'($d = 34.55$, $k_1 = 5.6$, $\eta = 13°$)

(a) $\eta = 6°$, $14°$($d = 34.55$, $k_1 = 6$, $k_2 = 10.5$)

(b) $\eta = 6°$, $18°$($d = 34.55$, $k_1 = 5$, $k_2 = 9.85$)

Fig. 19 Comparison of tooth profile with different rotation angles

of 'd' is selected based on the radius of the pitch circle (inner:31.9 mm, outer:34.8 mm) and is relatively limited depending on the requirement of the minimum outer rotor-radial thickness (4.1 mm). As the value of 'k_1' increases, the outer lobe is scaled in the direction of the x-axis, and the tooth thickness of the inner rotor increases and that of the outer rotor decreases as shown in Fig. 16. Figure 17 shows that as the value of 'k_2' increases, the outer lobe is scaled in the y-axis direction, so the tooth thickness of the inner rotor decreases and that of the outer rotor increases. Figure 18 shows that as the value of 'η' changes, the outer lobe shape has a different curvature. For example, Fig. 19 shows the comparison between the tooth profiles generated when $\eta = 6°$ and $\eta = 14°$ and the comparison between the tooth profiles generated when $\eta = 6°$ and $\eta = 18°$, given the same values

of 'd', 'k_1', 'k_2'. At this time, as the value of 'η' is increased from 6° to 14°, the lobe shape becomes more smooth, and
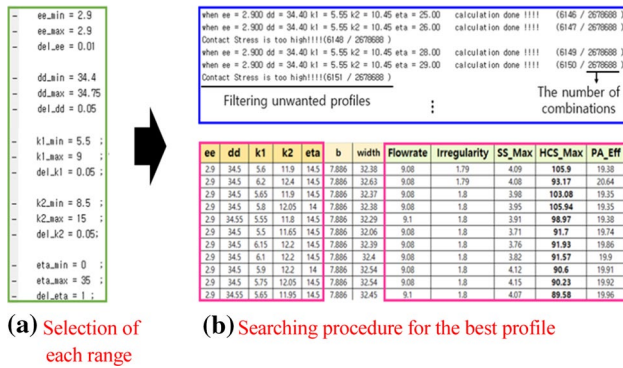
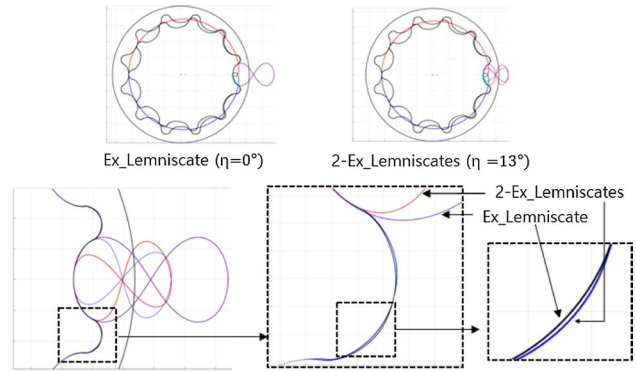**Fig. 20** Optimization process of gerotor using the multiple calculation program

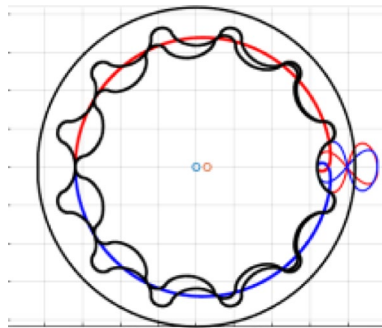**Fig. 22** Comparison of Ex_Lemniscate lobe shape with 2-Ex_Lemniscates lobe shape

Fig. 21 Optimal gerotor with 2-Ex_Lemniscates

Table 1 Comparison of performance parameters of optimal gerotors (Ex_Lemniscate and 2-Ex_Lemniscates lobe shapes)

Lobe type	Ex_Lemniscate	2-Ex_Lemniscates
Irregularity (%)	1.95	1.88 (3.6%↓)
Contact stress (MPa)	126.7	98.91 (27.8 MPa↓)
Specific slipping (%)	2.97	2.63 (11.4%↓)
Pressure angle (°)	18.91	17.51 (1.4° ↓)
Flow rate (cc/rev)	9.09	9.1 (0.1 cc/rev ↑)

then, as the value of 'η' is increased to 18°, the lobe shape becomes more angular.

3.2 Optimal Tooth Profile Selection Procedure by Automatic Calculation Program

Multi-calculation program, which automatically calculates performance parameters for all tooth profiles generated and performs filtering for tooth profiles that do not satisfy the target values of performance parameters, was developed. Range and interval of each design parameter are entered as follow: The numbers of teeth of inner and outer rotors of 11/12, the outer diameter of the outer rotor of 83.730 mm, the outer rotor-radial thickness of 4.1 mm, the gerotor thickness of 7.886 mm and the ranges of variable design parameters ('d', 'k1', 'k2', 'η') shown in Fig. 20a. Then, the program automatically calculates 2.6 million different tooth profiles and their performance parameters are calculated as shown in Fig. 20b. Gerotor profiles, which did not meet the requirements from the actual field (minimum flow rate of 9.05 cc/rev, maximum contact stress of 145 MPa), were filtered, and considering the order of priority relating to impact on noise (irregularity > contact stress > specific slipping > pressure

angle) [8], the optimal tooth profile with the 2-Ex_Lemniscates was selected as shown in Fig. 21.

In order to verify effect of the rotation algorithm on the gerotor performances, the optimal tooth profile with the Ex_Lemniscate curve not applying the rotation algorithm ('d' = 31.875 mm, 'k1' = 8.9, 'k2' = 13.8 and 'η' = 0°) was compared with the optimal tooth profile with 2-Ex_Lemniscates applying the rotation algorithm ('d' = 31.875 mm, 'k1' = 5.6, 'k2' = 10.85, and 'η' = 13°), as shown in Fig. 22. Their theoretical performance parameters were compared in Table 1, which shows irregularity, contact stress, specific slipping, and pressure angle decreased by 3.6%, 27.8 MPa, 11.4% and 1.4°, respectively. Since the number of tooth profile is multiplied by the number of 'η' by applying rotation algorithm, more various tooth profiles were generated, which contributed to the improvement of gerotor performances.

Compared to the theoretical performance parameters of the existing gerotor with 2-Ex_Cardioids, which is the optimal tooth profile among the previous studies, 2-Ex_Lemniscates show that irregularity, contact stress, specific slipping and pressure angle were decreased by 2.6%, 7.23 MPa, 6.7% and 1°, respectively as shown in Table 2. 2-Ex_Lemniscates profile generated has uniform clearance between inner and outer rotor, making profile rotationally symmetric as shown in Table 2.

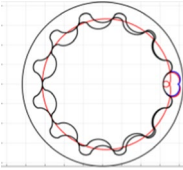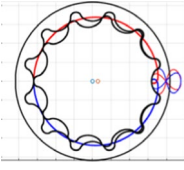**Table 2** Comparison of performance parameters of optimal gerotors (2-Ex_Cardioids and 2-Ex_Lemniscates)
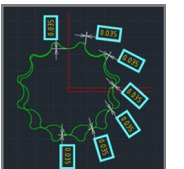
Lobe type	2-Ex_Cardioids	2-Ex_Lemniscates
Shape of gerotor		
Clearance between inner and outer rotor		
Clearance (mm)	0.035–0.043 mm	0.035 mm
Irregularity (%)	1.93	1.88 (2.6%↓)
Contact stress (MPa)	106.14	98.91 (7.2 MPa↓)
Specific slipping (%)	2.82	2.63 (6.7%↓)
Pressure angle (°)	18.51	17.51 (1.0° ↓)
Flow rate (cc/rev)	9.1	9.1 (-)

Fig. 23 Prototype of the oil pump with the optimal gerotor with the 2-Ex_Lemniscates

4 Performance Test

In general, there are flow and mechanical noises to be handled out in gerotor oil pump, but this study focuses on comparing the effect of noise by changing the flow characteristic caused by inner lobe shape automatically generated according to the outer lobe shape using lemniscate curve.

So, it was requested to a company that could measure flow rate, pressure pulse, torque, and noise in the same situation such as the actual operating environment shown in Fig. 23, and as a result, it was possible to accurately compare and analyze oil pumps designed with previous lobes.

In order to verify superiority of the optimal gerotor with the 2-Ex_Lemniscates lobe shape, the oil pump prototype including inner rotor, outer rotor, housing and cover was manufactured as shown in Fig. 22, and its performance test was conducted. The gerotor is rotated by the power of the
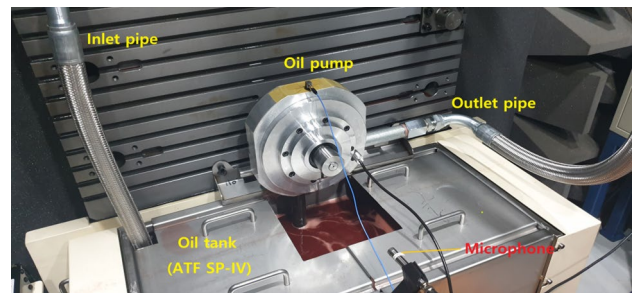

Fig. 24 Experimental apparatus for performance test of oil pump
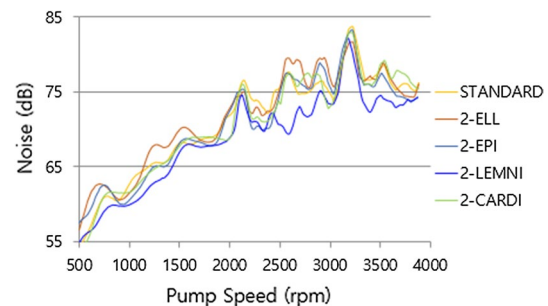

Fig. 25 SPL of the new oil pump and the existing pumps

driving motor, and the temperature of the working fluid (85 °C) is kept constant by the cooling water system. Target noise was measured through a noise measurement microphone 30 cm away from the oil pump as shown in Fig. 24. Flowrate measurement checked the amount of the exhausted auto transmission fluid (ATF). The ATF with 1 bar was taken in from the oil tank and transferred to the inlet pipe, and it was discharged through the outlet pipe at 16 bar.

The performance test was conducted at the rotational speed from 500 up to 5000 rpm, and the performance of the oil pump was mainly derived at the rotational speed from 2000 to 3000 rpm, which is used to determine the performance of automatic transmission oil pumps in the actual field. Noise of the new oil pump was compared with that of the existing standard oil pump used in the field, as well as the previous optimal gerotors (2-Ellipses, 2-Ex_Cardioids and 2-Ex_Epitrochoids).

Sound pressure levels (SPL) in the range from 500 to 4000 rpm were shown in Fig. 25. The minimum, maximum SPLs and the average SPL in the range from 2000 to 3000 rpm of the four oil pumps (2-Ellipses, 2-Ex_Cardioids and 2-Ex_Epitrochoids and 2-Ex Lemniscates) were compared with the existing standard oil pump as shown in Table 3. The average SPL of the new oil pump with 2-Ex_Lemniscates (71.85 dB), which was the lowest value, was decreased by 3.75%, and the SPL of the new one was lower

Table 3 Comparison of SPLs between existing oil pump 1(standard) and other pumps

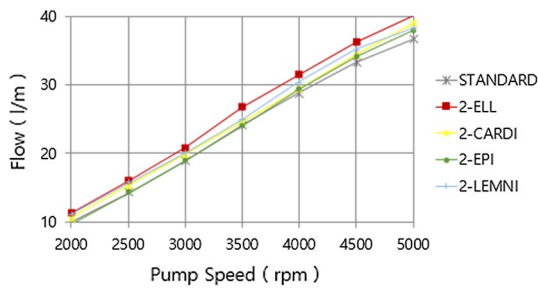|	Noise (dB)		
	Min	Max	Average (2000–3000 rpm)
Existing oil pump 1 (Standard)	71.53	77.64	74.93
Existing oil pump 2 (2-Ellipses)	71.94 (0.40 ↑)	79.61 (1.97 ↑)	75.84 (1.60%↑)
Existing oil pump 3 (2-Ex_Cardioids)	68.52 (3.01 ↓)	77.51 (0.13 ↓)	74.32 (0.43%↓)
Existing oil pump 4 (2-Ex_Epitrochoids)	69.95 (1.58 ↓)	78.9 (1.26 ↓)	74.46 (0.24%↓)
New oil pump (2-Ex_Lemniscates)	68.4 (3.14 ↓)	75.15 (2.49 ↓)	71.85 (3.75%↓)

Fig. 26 Flowrate of the new oil pump and the existing pumps (2000–5000 rpm)

Table 4 Comparison of flowrates between existing oil pump 1 (standard) and other pumps

	Flow rate (L/min)		
	2000 rpm	2500 rpm	3000 rpm
Existing oil pump 1 (Standard)	9.94	14.23	18.97
Existing oil pump 2 (2-Ellipses)	11.2 (12.7% ↑)	15.97 (12.3% ↑)	20.8 (9.7% ↑)
Existing oil pump 3 (2-Ex_Cardioids)	10.59 (6.6% ↑)	15.27 (7.3% ↑)	19.86 (4.7% ↑)
Existing oil pump 4 (2-Ex_Epitrochoids)	9.69 (2.5% ↑)	14.23 0.00%	18.84 (0.7% ↑)
New OIL pump (2-Ex_Lemniscates)	11.04 (11.1% ↑)	15.71 (10.4% ↑)	20.13 (6.1% ↑)

by 3.14 dB in the minimum and by 2.49 dB in the maximum, this means the developed tooth profile has contributed to the improvement of noise reduction.
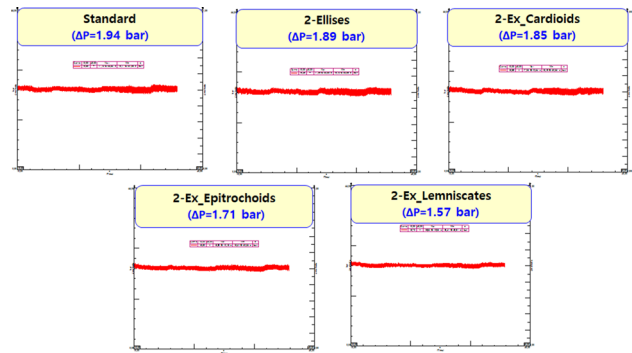

Fig. 27 Pressure irregularity of the new oil pump and the existing pumps

Table 5 Comparison of pressure irregularities between existing oil pump 1(standard) and other pumps

	P_{min}(bar)	P_{max}(bar)	ΔP (bar)
Existing oil pump 1 (Standard)	15.17	17.13	1.94
Existing oil pump 2 (2-Ellipses)	15.19 (0.02 bar↑)	17.06 (0.07 bar↓)	1.89 (2.5%↓)
Existing oil pump 3 (2-Ex_Cardioids)	15.18 (0.01 bar↑)	17.02 (0.11 bar↓)	1.85 (4.6% ↓)
Existing oil pump 4 (2-Ex_Epitrochoids)	15.31 (0.14 bar↑)	16.98 (0.15 bar↓)	1.71 (11.8% ↓)
New oil pump (2-Ex_Lemniscates)	15.41 (0.24 bar↑)	16.99 (0.14 bar↓)	1.57 (19.1%↓)

The flowrates from 2000 to 5000 rpm were shown in Fig. 26, and the flowrates of the five oil pumps (2-Ellipses, 2-Ex_Cardioids and 2-Ex_Epitrochoids and 2-Ex Lemniscates) were compared with the existing standard oil pump as shown in Table 4 at 2000 rpm, 2500 rpm, and 3000 rpm. The oil pump with the 2-Ellipses showed the highest flowrate, followed by that with 2-Ex_Lemniscates, 2-Ex_Cardioids and 2-Ex_Epitrochoids, and the oil pumps with 2-Ellipses and 2-Ex_Lemniscates showed significantly higher flowrates than the others.

In order to improve noise reduction of gerotor oil pump, it is important to reduce pressure irregularity ($P_{max} - P_{min} = \Delta P$). The pressure data at the outlet were shown in Fig. 27, and the irregularity was compared in Table 5. The irregularity of the 2-Ex_Lemniscates was 1.57 bar, which is decreased by 19.1% than that of the existing oil pump (1.94 bar), which showed a significant improvement.

5 Conclusion

This study proposed the optimal design of gerotor profile with 2-Ex_Lemniscates lobe shape to apply it to miniaturized auto-transmission oil pump of automobile (outer rotor diameter: 83.730 mm) and verified that the optimal gerotor has high flow-rate and also sufficiently lower pressure irregularity and noise levels by conducting performance test, compared to the previous pumps: existing oil pump 1, 2-Ellipses, 2-Ex_Cardioids and 2-Ex_Epitrochoids oil pump. The results of this study were summarized as follows.

1. 2-Ex_Lemniscates; 2-expanded lemniscates curve, was developed as a new lobe shape for lower irregularity and noise, and theoretical equations for generating a rotor profile with this curve used as the tooth profile of the outer rotor were derived.
2. The new algorithm has removed 'cusp' generated in outer rotor and made uniform clearance between outer and inner rotor by applying translational movement of the x and y axes along with the expansion and rotation.
3. The automatic program that automatically generates the various tooth profiles according to the inputted design parameters and calculates the theoretical performance parameters was developed
4. The multi-calculation program for optimization of tooth profile was developed using Matlab, and then, the optimal gerotor with the 2-Ex_Lemniscates lobe shape was selected ('d' = 31.875 mm, 'k1' = 5.6, 'k2' = 10.85, and 'η' = 13°); The optimal gerotor with a 2-Ex_Lemniscates lobe shape shows that the theoretical irregularity, contact stress, specific slipping and pressure angle of the optimal tooth profile were decreased by 2.6%, 7.23 MPa, 6.7% and 1°, respectively, compared to the previous optimal gerotor with 2-Ex_Cardioids.
5. Compared to the previous optimal oil pump with 2-Ex_Cardioids, the new oil pump showed that the flow rate at 2500 rpm was increased by about 2.9%, and average SPL (2000–3000 rpm) and pressure irregularity were decreased by 3.3% and 16.9%, respectively.

References

1. Hsieh, C., & Hwang, Y. (2006). Geometric design for a gerotor pump with high area efficiency. *ASME Journal of Mechanical Design, 129*(12), 1269–1277.
2. Ravari, M. K., Forouzan, M. R., & Moosavi, H. (2012). Flow irregularity and wear optimization in epitrochoidal gerotor pumps. *Meccanica, 47*, 917–928. https://doi.org/10.1007/s11012-011-9473-6(4)
3. Bonandrini, G., Mimmi, G., & Rottenbacher, C. (2012). Design and simulation of meshing of a particular internal rotary pump. *Mechanism and Machine Theory, 49*, 104–116.
4. Sang X, Zhou X, Liu X (2015) Performance optimization of an oil ellipse gerotor pump for automotive engine. In: Proceedings of the 5th international conference on advanced design and manufacturing engineering
5. Gamez-Montero, P. J., Castilla, R., Codina, E., Freire, J., Morató, J., Sanchez-Casas, E., & Flotats, I. (2017). GeroMAG: in-house prototype of an innovative sealed, compact and non-shaft-driven gerotor pump with magnetically-driving outer rotor. *Energies, 10*(4), 435.
6. Rituraj F, Vacca A (2019) Modelling and validation of tooth tip leakages in gerotor pumps. In: Proceedings of the ASME-JSME-KSME 2019 8th joint fluids engineering conference. Volume 1: fluid mechanics. San Francisco, California, USA. July 28–August 1, 2019. V001T01A044. ASME
7. Cao, W., Liu, Y., Dong, J., Niu, Z., & Shi, Y. (2019). Research on pressure pulsation characteristics of gerotor pump for active vibration damping system. *IEEE Access, 7*, 116567–116577. https://doi.org/10.1109/ACCESS.2019.2936489
8. Lee, S. H., Kwak, H. S., Han, G. B., & Kim, C. (2019). Design of gerotor oil pump with 2-expanded cardioids lobe shape for noise reduction. *Energies, 12*(6), 1126.
9. Tessari, F., Galluzzi, R., & Amati, N. (2019). Efficiency-driven design methodology of gerotor hydraulic units. *ASME Journal of Mechanical Design, 142*(6), 063501.

Changhyun Lee is a master's course in the School of Mechanical Engineering, Pusan National University, Pusan, Korea. His research interests include finite element analysis.

Hyoseong Jang is a doctor's course in the School of Mechanical Engineering, Pusan National University, Pusan, Korea. He received master's degree of creative engineering system at Pusan National University in 2015. His major research fields are gear design and computational fluid dynamics.

Hyoseo Kwak received M. S. degree in School of Creative Engineering and Ph.D. degree in Mechanical Convergence Technology, Pusan National University, Korea, in 2012, 2014 and 2017. She is currently an assistant professor in. YoungSan University. Her research fields extend into machine design and FEM simulation.

Chul Kim is a Professor of mechanical engineering at Pusan National University, Korea. He received doctoral degree of mechanical engineering at Pusan National University in 1977. His major research fields extend into FEM simulation (structure, dynamic and fluid analysis), optimal structural design, CAD/CAM.

Gunyoung Park is a doctor's course in the School of Mechanical Engineering, Pusan National University, Pusan, Korea. He received master's degree of Mechanical convergence technology at Pusan National University in 2018. His major research fields are composites and finite element analysis.